Vibrational properties of quasi-two-dimensional colloidal glasses with varying interparticle attraction

Matthew D. Gratale,[1] Xiaoguang Ma,[1,2] Zoey S. Davidson,[1] Tim Still,[1] Piotr Habdas,[3,*] and A. G. Yodh[1,†]
[1]*Department of Physics and Astronomy, University of Pennsylvania, Philadelphia, Pennsylvania 19104, USA*
[2]*Complex Assemblies of Soft Matter, CNRS-Solvay-UPenn UMI 3254, Bristol, Pennsylvania 19007-3624, USA*
[3]*Department of Physics, Saint Joseph's University, Philadelphia, Pennsylvania 19131, USA*
(Received 30 June 2016; published 20 October 2016)

We measure the vibrational modes and particle dynamics of quasi-two-dimensional colloidal glasses as a function of interparticle interaction strength. The interparticle attractions are controlled via a temperature-tunable depletion interaction. Specifically, the interparticle attraction energy is increased gradually from a very small value (nearly hard-sphere) to moderate strength ($\sim 4k_BT$), and the variation of colloidal particle dynamics and vibrations are concurrently probed. The particle dynamics slow monotonically with increasing attraction strength, and the particle motions saturate for strengths greater than $\sim 2k_BT$, i.e., as the system evolves from a nearly repulsive glass to an attractive glass. The shape of the phonon density of states is revealed to change with increasing attraction strength, and the number of low-frequency modes exhibits a crossover for glasses with weak compared to strong interparticle attraction at a threshold of $\sim 2k_BT$. This variation in the properties of the low-frequency vibrational modes suggests a new means for distinguishing between repulsive and attractive glass states.

DOI: 10.1103/PhysRevE.94.042606

I. INTRODUCTION

Many properties of glasses depend on the interactions between constituent particles [1–25]. In colloidal glasses with high packing fraction, for example, two qualitatively different states have been observed that depend on the strength of the short-range attraction between particles [9–19]. Glasses with weak interparticle attraction reside in a so-called "repulsive" glass state, and glasses whose constituents experience strong interparticle attraction reside in an "attractive" glass state. The existence of these two states has been confirmed by experiment [10–13,15,19] and simulation [3,9,20,21], and the constituent particle dynamics in repulsive versus attractive glasses have also been observed to be different [9–15]. Most previous studies, however, tend to compare these properties in two extreme limits, e.g., hard-sphere glasses versus glasses with very strong interparticle attraction. Indeed, to our knowledge, few studies have explored the crossover behavior of colloidal glasses as the interparticle attraction strength is gradually increased from nearly hard-sphere to strongly attractive.

The differences in properties between glassy states arise from different mechanisms of dynamical arrest. In repulsive glasses, the particle dynamics slow down due to local crowding. Particles are trapped in entropic "cages" created by neighboring particles. By contrast, in attractive glasses, in addition to local crowding, the particle dynamics are slowed even more as a result of strong interparticle attractions. Further, the heterogeneous dynamics of attractive glasses occurs over a larger range of length and time scales compared to repulsive glasses [15], and the cooperative rearrangement regions (CRRs) in repulsive glasses are string-like, while in attractive glasses CRRs are compact [15]. These differences in dynamical arrest mechanism also lead to variation of bulk rheological properties, for example, the phenomenon of two-step yielding in attractive glasses [23].

Theory supports some of these observations. Mode coupling theory (MCT) predicts that densely packed glasses with short-range interparticle attraction have two distinct arrested states [1,6,16–18]. MCT also predicts behavior at the crossover between repulsive and attractive glass states. In particular, the transition predicted by MCT [1,6,16–18] is characterized by discontinuous jumps in various quantities with respect to an attractive potential minimum. The Debye-Waller factor, or the nonergodicity parameter, for example, is a transition indicator and was found to exhibit a jump as a function of reduced temperature k_BT/u_0, where u_0 is the depth of the interparticle potential well, i.e., the attraction strength [17].

In this contribution we investigate the phonon modes and particle dynamics of glasses in the transition region. In general, disordered solids such as glasses show an excess of low-frequency vibrational modes. This excess is not predicted by the Debye model of simple crystals and is known as the "boson" peak [26]. The boson peak is commonly exhibited at low frequencies by a plot of the vibrational Density of States [$D(\omega)$] scaled by the expected Debye behavior, i.e., $D(\omega)/\omega^{d-1}$, where d is the sample dimension. The presence and height of the boson peak is used as an indicator of the glass transition [27–32]. Experiment and simulation have also found that these low-frequency modes are quasilocalized and display enhanced participation in regions prone to rearrangements [27,33–46].

Previously the behavior of the vibrational $D(\omega)$ was shown to vary when crossing from an attractive glass state to the gel state [22]; in this case, traditional order parameters did not prove useful for characterizing the transition. Note, however, this previous work studied vibrational phonons in disordered materials as a function of packing fraction with a constant, strong interparticle attraction. It was observed that sparsely packed gel-like states have an excess of low-frequency modes compared to densely packed attractive glass states. The excess

*Corresponding author: phabdas@sju.edu
†Corresponding author: yodh@physics.upenn.edu

of modes, in this case, arose largely from localized vibrations involving small clusters of particles. Stimulated by these findings, and previous work on glasses, the present contribution explores how the character of vibrational modes changes in the transition region between repulsive and attractive glasses at constant packing fraction.

To this end, we vary the interparticle attraction strength between colloidal particles confined in quasi-two-dimensional (2D) sample cells using temperature-tunable depletant micelles [47,48]. The vibrational properties of the glass are measured as a function of temperature, at approximately constant packing fraction, as the system evolves from a nearly hard-sphere glass to an attractive glass. Our expectation is that vibrational signatures will distinguish the two glassy regimes, and indeed we observe evidence of a crossover transition from the repulsive glass to the attractive glass at an interparticle attraction strength of approximately $2k_BT$. As the interparticle attraction is increased through this regime, the $D(\omega)$ of the system at low frequencies decreases and saturates for attractions strengths greater than $\sim 2k_BT$. Moreover, these low-frequency modes exhibit a quasilocalized character for attractions below $\sim 2k_BT$ and a more extended character for attractions above $\sim 2k_BT$. The observations suggest that the variations of the vibrational $D(\omega)$ could serve as an indicator of repulsive-to-attractive transitions associated with colloidal glasses. The experimental results should stimulate new theoretical and simulation investigation of vibrations in glasses, and, in combination, experiment and theory could provide further insight into these systems.

II. EXPERIMENTAL METHODS

Samples solutions of silica spheres with diameters 1.2 μm (Bangs Laboratiories) and 1.57 μm (Thermo Scientific) are prepared with a 1:1 number ratio. The polydispersity estimated by the manufacturer is 10%–15% for the small particles and is 2.5% for the large particles. When the spheres are densely packed, the size ratio ($\sim$1.3) and number ratio help frustrate crystallization [49–51], and thus can be used to create geometrically disordered colloidal glasses. The particles reside in a solution containing 44 mM hexaethylene glycol monododecyl ether ($C_{12}E_6$) surfactant micelles and 17 mM NaCl in water. The negatively charged silica spheres in water are well approximated as hard spheres due to the strong screening by the added salt. The use of $C_{12}E_6$ micelles as depletants provides a temperature tunable depletion interaction, wherein the strength of the interparticle attraction increases as sample temperature is increased due to the changing length distribution of the rodlike micelles [48].

We use wedge cells in this experiment to create large quasi-2D domains (>8 mm^2 in area) of densely packed colloidal suspension. The construction of the wedge cells is adapted from the procedure by Gerbode *et al.* [52]. The angle of the wedge $\sim 8 \times 10^{-4}$ degrees is shallow enough so that over the field of view (60 μm by 60 μm) the cell walls are effectively parallel. We first inject 5 μl of sample solution with a volume fraction of approximately 0.1 into the wedge cell using a pipette. Then we seal the cells peripherally with optical glue (Norland 65) cured for 30 min under a UV lamp. The completed sample cells are placed vertically on the bench with the wedge pointing down for two days. Silica spheres sediment to the wedge side and form large domains of densely packed colloidal glass with a packing fraction $\phi = 0.82$.

The sample cell is placed on the stage of an inverted microscope (Zeiss Axiovert 135) and viewed from below using bright field microscopy. With a 100$\times$ oil immersion objective and a 2.5$\times$ internal magnifier, $N_{\rm tot} \approx 1700$ particles are in the field of view. Videos of particle motion are recorded at 100 frames per second for 100 000 frames using a monochrome CMOS camera (EoSens1362, Mikrotron). Commercial image acquisition software (XCAP, EPIX) is used to control the camera and stream video frames to the hard drive of a host computer. Particle trajectories are obtained from the video using standard particle-tracking algorithms [53] with an accuracy of $\sim$10 nm in particle positions. Videos were taken at 12 sample temperatures ranging from 23 °C to 35 °C with 1 °C increments obtained using an objective heater (Bioptechs).

We calculate vibrational modes of the colloidal samples from particle trajectories [27,28,54]. To this end, we follow the procedure originally suggested with some corrections developed later that improve upon these procedures; all of these techniques and corrections are described in detail in previous work [22,27,28,54–62]. Briefly, we first calculate the time-averaged covariance matrix $\langle C_{ij} = u_i(t)u_j(t) \rangle_t$, where $u_i(t)$ are particle displacements from their average positions. In the harmonic approximation, the covariance matrix is directly related to the matrix of effective spring constants, K, connecting particles in an undamped shadow system, i.e., by $(C^{-1})_{ij}k_BT = K_{ij}$. Δ is the dynamical matrix of this shadow system and is related to K by $\Delta_{ij} = K_{ij}/m_{ij}$, where $m_{ij} = \sqrt{m_i m_j}$ is the reduced mass and m_i is the mass of particle i. From the eigenvalues of the dynamical matrix the squared frequencies of vibrational modes of the system, ω^2, can be calculated. The corresponding eigenvector, $\vec{e}_i(\omega)$, represents the displacement amplitudes of the given vibrational mode at frequency ω for the particle i.

III. RESULTS AND DISCUSSION

A. Pair correlation functions

We measure the sample pair correlation function, $g(r)$, at different temperatures. This measurement enables us to ascertain radial structure variation as a function of attraction strength. In Fig. 1 we show measured $g(r)$ at six temperatures. The results exhibit structural features commonly observed in bidisperse dense colloidal suspensions. Specifically, three peaks are observed near the first shell of immediate neighbors; these peaks are due to small-small, small-large, and large-large particle separations, respectively. The broad shoulder of the first peak is due in part to the large polydispersity (10%–15%) of the small particles; on the other hand, the third peak due to the contacts between large particles has a much narrower shoulder due to the uniformity of the large particles. The measured $g(r)$ show little change as the strength of interparticle attraction increases. Thus, measurements of pair correlation functions do not appear to capture any feature that reveals a crossover transition from repulsive glass to attractive glass (i.e., within our signal-to-noise); note that small structure changes in the radial functions have been discerned in other

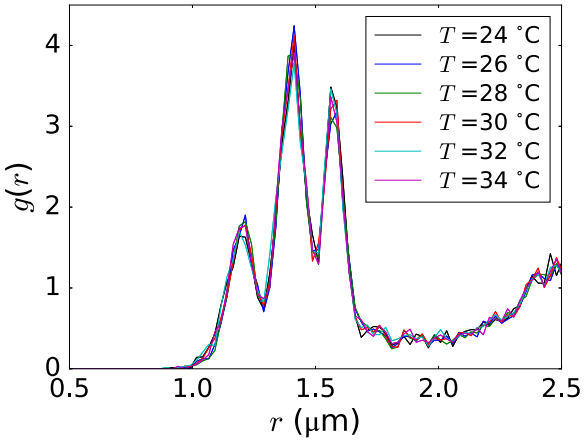

FIG. 1. Pair correlation function, $g(r)$, for a representative subset of temperatures (24 ° C, 26 ° C, 28 ° C, 30 ° C, 32 ° C, and 34 ° C).

systems [11,13]. At high packing fractions the pair correlation function generally depends on the particle interaction at very short range, and, within our experimental resolution, this short-range repulsive part of the interparticle potential is similar for particles in both the repulsive and attractive glasses. This observation is consistent with the classic work of Weeks *et al.* [63] and recent computer simulation results [5,64]. Absent obvious structural effects, we shift to explore dynamic features to characterize the transition, including mean-squared displacement, the vibrational modes, and the phonon density of states.

B. Mean-squared displacement

We first study the particle mean-squared displacements (MSD). We plot the measured MSD, $\langle \Delta r^2(\Delta t) \rangle$, at different temperatures in Fig. 2. The plateaus at intermediate lag time scale (Δt) exhibited by the MSDs are signatures of arrested particle dynamics and are observed for all temperatures. Notice also that the values of the measured MSDs decrease monotonically with increasing temperature at all lag times. To better demonstrate this dependency on temperature, we pick out the MSD values at a specific lag time, $\Delta t = 21.8$ seconds, marked by the dash line in Fig. 2(a), and we plot them as a function of temperature, as shown in Fig. 2(b). These MSD data as a function of temperature clearly show two linear regions with different slopes in Fig. 2(b). The MSD value decreases at a fast rate when the temperature is below 26 ° C, and then saturates above 28 ° C. Variation in the region between the two temperatures suggests the existence of a crossover transition from repulsive to attractive glass.

We estimate the interparticle potentials from experimentally determined pair correlation functions measured in the dilute concentration regime [48] using liquid structure theory [65,66]. Following previous work with this system class [11,15,67], we utilize the interaction potential estimate in the dilute regime as a surrogate for the (unmeasured) potential in the dense regime. Thus, herein we report the potential measured in dilute regime (which is unambiguously measured). Thus, in Fig. 2(b) we also provide the measured attraction strength, i.e., the depth of the attractive potential $|U_{\min}|$, on the

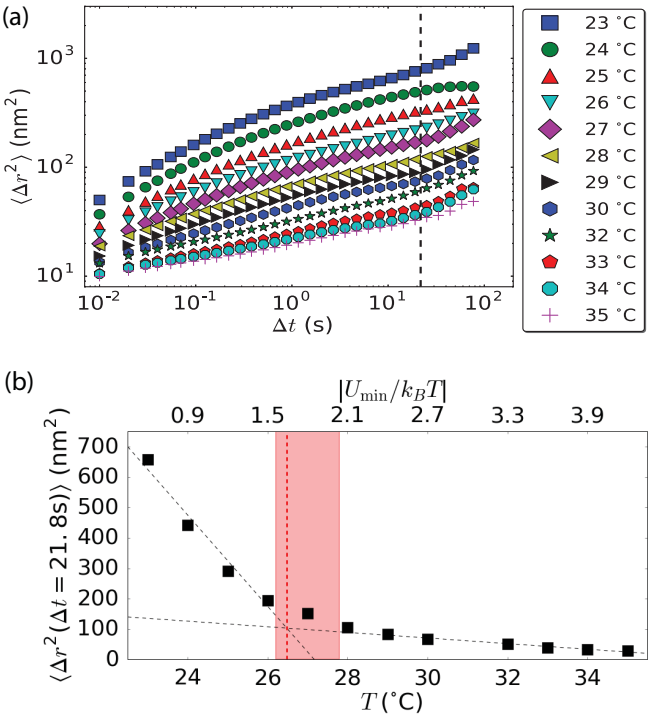

FIG. 2. (a) Mean-squared displacement, $\langle \Delta r^2(\Delta t) \rangle$, measured at different temperatures. Dashed line represents lag time $\Delta t = 21.8$ s. (b) Measured $\langle \Delta r^2(\Delta t) \rangle$ at $\Delta t = 21.8$ s as a function of temperature. This behavior is similar for all lag times between 0.1 s and 100 s. The top horizontal axis indicates the attraction strength $|U_{\min}(T)/k_BT|$ measured in dilute particle suspensions at the temperatures indicated on the bottom horizontal axis [48]. The black dash lines are linear fitting of data measured at low and high temperatures, corresponding to the repulsive and attractive glasses, respectively. The red dashed line represents the intersection of the two fits. The shaded red region represents the range of temperatures and attraction strengths at which the repulsive-to-attractive glass crossover could reasonable occur. Error bars are smaller than the size of the symbols.

upper horizontal axis. Using the attraction strength variation with temperature, the crossover transition from repulsive to attractive glass is estimated to be between $1.5k_BT$ and $2k_BT$.

Lastly, we note that MSD values at the shorter time scales (less than $\Delta t \approx 10$ s) reflect the free volume size available to the "caged" particle. Thus, decreasing MSD in this regime indicates shrinking free volumes. In a near-jammed packing with only repulsive interactions, the free volume is determined by the local packing condition [68]. In our experiments, interestingly, the reduction in cage size is due solely to the emerging attractive force. The attraction between contacting particles hinders particle motion, and an attraction strength of $2k_BT$ seems to be sufficient to saturate the available volume to particles. While the transition is comparatively sharp, we definitely do not observe a discontinuous jump in the MSDs as a function of attraction strength, as was found in the Debye-Waller factors calculated by MCT [17].

C. Vibrational phonon behavior

To further explore the transition from the repulsive glass state to the attractive glass state, we calculated the

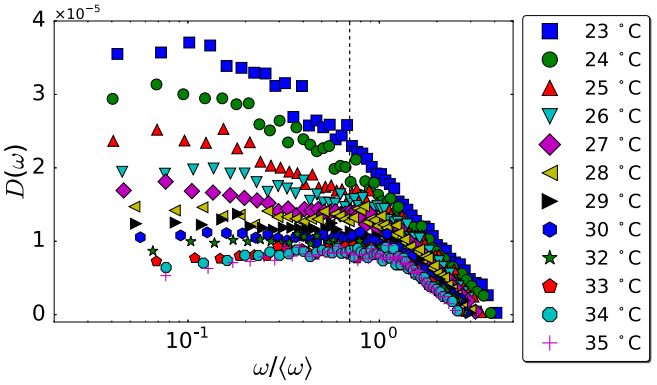

FIG. 3. Vibrational density of states, $D(\omega)$, versus scaled phonon frequency, $\omega/\langle\omega\rangle$, in semi-log plot. Dashed line represents $\omega/\langle\omega\rangle = 0.7$.

vibrational phonon modes of these colloidal glass samples with varying attractive interaction strength between constituents. The resulting distribution of the $D(\omega)$ varies as the strength of interparticle attraction increases (see Fig. 3). Specifically, we observe that the $D(\omega)$ of the low-frequency modes (i.e., with mode frequencies ω scaled by the sample mean frequency $\langle\omega\rangle$ such that $\omega/\langle\omega\rangle < 0.7$) decreases as the strength of the attraction grows. This effect is clearly observed when the $D(\omega)$ is plotted on a log scale as a function of the phonon frequency scaled by the mean frequency of each sample, $\omega/\langle\omega\rangle$ (Fig. 3). Qualitatively, the value of $D(\omega)$ at low frequencies decreases monotonically with increasing temperature and attraction strength. To quantify this effect, we calculated the density of states and its average, $D(\omega)$, $\langle D(\omega)\rangle$, respectively, for modes with $\omega/\langle\omega\rangle < 0.7$ (Fig. 4).

Using these definitions for the mode ranges, we observe trends that are similar to that found for the MSD. We find that $\langle D(\omega)\rangle$ for modes with $\omega/\langle\omega\rangle < 0.7$ decreases monotonically in the low-temperature (low attraction) regime and plateaus

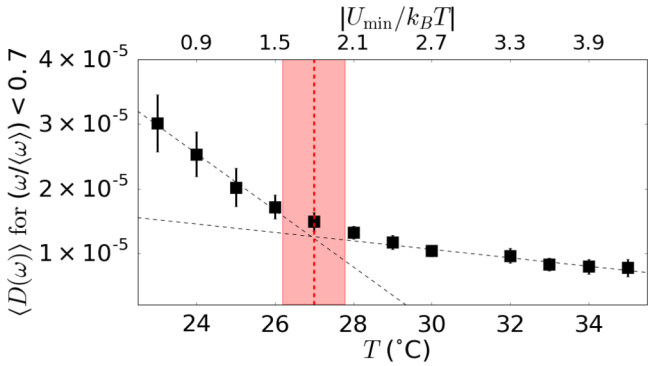

FIG. 4. The average density of states, $\langle D(\omega)\rangle$, for modes with $(\omega/\langle\omega\rangle) < 0.7$, for all temperatures, T. The top horizontal axis indicates the attraction strength $|U_{\min}(T)/k_BT|$ measured in dilute particle suspensions at the temperatures indicated on the bottom horizontal axis [48]. Black dashed lines are linear fits to the two regimes (monotonic decrease and plateau), corresponding to the two glass states (repulsive and attractive). The red dashed line represents the intersection of the two fits. The shaded red region represents the range of temperatures and attraction strengths at which the repulsive-to-attractive glass crossover could reasonably occur.

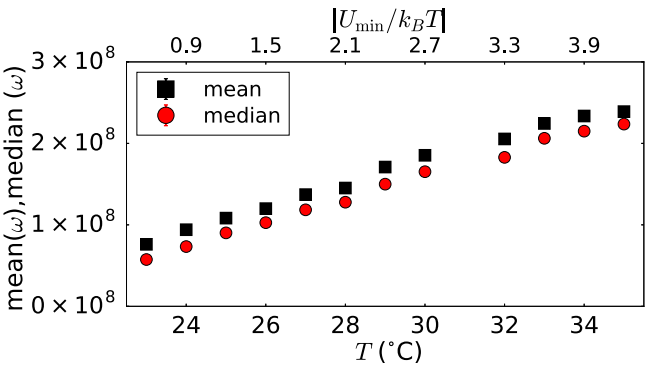

FIG. 5. Mean (black squares) and median (red circles) phonon frequencies vs temperature. Error bars are smaller than the size of the symbols.

at strong attraction strength. Specifically, we observe that $\langle D(\omega)\rangle$ for modes with $\omega/\langle\omega\rangle < 0.7$ plateaus at attraction strengths greater than $2k_BT$. This provides further evidence of a crossover transition between states of the glass that occurs when the interparticle attraction strength is approximately $2k_BT$.

By contrast, the mean and median phonon frequencies of each sample increased monotonically and smoothly with temperature (Fig. 5). No evidence of a crossover transition is apparent for these parameters. Again, this continuous increase in the mean and median frequencies is consistent with the fact that the interparticle attraction strength increases linearly with temperature. We expect that with increasing attraction strength, the effective spring constants, k, between all pairs of particles increase. Increasing spring constants leads to increasing frequencies since $\omega \propto \sqrt{k}$. The continuous increase of the mean frequencies is evidence that the strength of the interparticle bonds is continuously increasing. Therefore, the plateaus observed in the other measured and calculated quantities are not caused by a saturation in the interparticle bond strength, but are rather due to a saturation of the dynamical arrest in the system.

Last, we explored the localized versus extended nature of the low-frequency modes. We computed the so-called mode participation ratio for this purpose. The participation ratio is defined as $P_R(\omega) = [\sum_\alpha e^2_{\alpha x}(\omega) + e^2_{\alpha y}(\omega)]^2/[N_{\rm tot}\sum_\alpha e^4_{\alpha x}(\omega) + e^4_{\alpha y}(\omega)]$, where $e_{\alpha x}(\omega)$ and $e_{\alpha y}(\omega)$ are the x and y eigenvector components for particle α, respectively. $P_R(\omega) \sim 1/N$ for a localized mode; $P_R(\omega) \sim O(1)$ for an extended mode. Following convention, we refer to frequencies with a participation ratio below 0.2 as localized, and frequencies with participation ratio above 0.2 as extended [34]. At interparticle attractions greater than $2k_BT$, many more extended modes at low frequencies are observed that are not found in samples with weaker interparticle attractions (Fig. 6).

Representative low-frequency modes of a repulsive glass and an attractive glass are presented in Fig. 7(a) and 7(b), respectively. These representative modes help visualize the effect that in repulsive glasses the modes at low frequencies are quasilocalized, whereas in attractive glasses extended collective motion is found throughout the sample. The low-frequency behavior of the repulsive glasses studied here are consistent with those previously studied [27,33,34,37–41], specifically

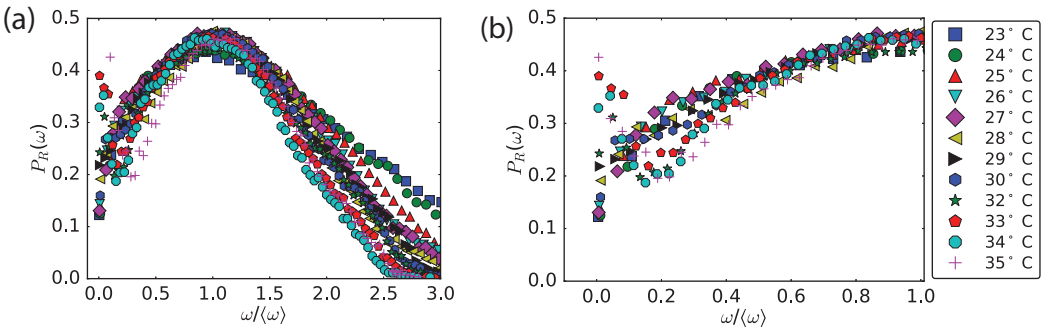

FIG. 6. (a) Participation ratio, $P_R(\omega)$, for all temperatures versus scaled frequency, $\omega/\langle\omega\rangle$. (b) $P_R(\omega)$ of modes with $\omega/\langle\omega\rangle < 1$.

that the presence of quasilocalized modes is found. The extended modes observed here in the low-frequency modes of attractive glasses is likely due to the strong interparticle bonds in attractive glasses. As one particle moves, it pulls its neighbors with it, which in turn pull their neighbors. This same reasoning can be used to account for the larger size of cooperative rearrangement regions (CRRs) observed in attractive glasses compared to CRRs observed in repulsive glasses [15].

To quantify the presence of these extended low-frequency modes in attractive glasses, we examined the lowest 100 modes, and we defined modes that have a participation ratio larger than 0.2 as extended. By measuring the number (within the lowest 100 modes) of modes that are extended (Fig. 8), we again see the same trend as observed in all of our other data: the number of extended modes plateaus at attraction strengths above $2k_BT$. Thus, another quantity associated with the phonons exhibits a crossover trend that saturates when the attraction strength is larger than $2k_BT$. Again, this saturation effect appears to signify the transition from the repulsive glass state to the attractive glass state.

IV. CONCLUSION

In summary, we experimentally studied the vibrational phonons of 2D colloidal glasses with increasing attraction strength, and presented evidence that the transition within glassy colloids occurs from a repulsive glass state to an attractive glass state. From the data, it appears that the crossover interparticle attraction strength is $2k_BT$. This transition is signified by changes in the distribution of the $D(\omega)$, as well in the saturation of the particle dynamics. We observe that repulsive glasses have an excess of low-frequency modes compared to attractive glasses. Furthermore, the motion of a majority of the lowest frequency modes in attractive glasses is spatially extended, wherein in repulsive glasses the motion at low frequencies is quasilocalized. We also observed that particle dynamics decreased monotonically with increasing attraction strength, but that the particle dynamics are saturated for attraction strengths larger than $2k_BT$, signifying the system is reaching a point of maximal arrest. The quantities measured herein did not display a discontinuous jump at the transition point like those calculated from MCT, but they did display a noticeable change in behavior at the transition point.

Future work should investigate if the glass reentrance phenomenon observed in 3D experiments [10–13] is also present in 2D samples. This phenomenon is found when the attraction strength between particles increases, and the system transitions from the repulsive glass state to the fluid state. As interparticle attraction strength increases further, the system undergoes a second transition from the fluid state to the attractive glass state. To date, reentrance has not been

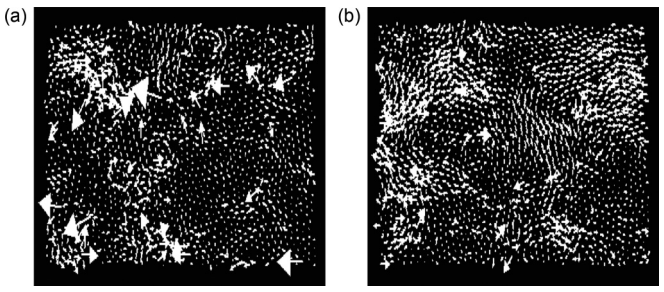

FIG. 7. (a, b) Vector displacement plots of representative low-frequency modes in a repulsive glass ($T = 23^\circ$ C, $|U_{\min}| = 0.5k_BT$) and an attractive glass ($T = 35^\circ$ C, $|U_{\min}| = 4.2k_BT$), respectively.

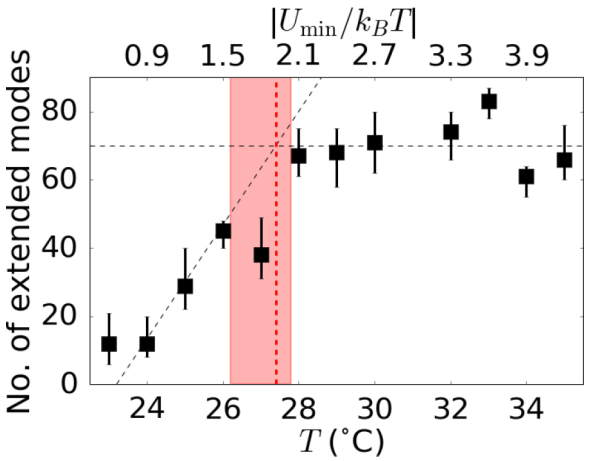

FIG. 8. Number of extended modes [$P_R(\omega) > 0.2$] of the lowest 100 modes. The top horizontal axis indicates the attraction strength $|U_{\min}(T)/k_BT|$ measured in dilute particle suspensions at the temperatures indicated on the bottom horizontal axis [48]. Black dashed lines are linear fits to the two regimes (monotonic decrease and plateau), corresponding to the two glass states (repulsive and attractive). The red dashed line represents the intersection of the two fits. The shaded red region represents the range of temperatures and attraction strengths at which the repulsive-to-attractive glass crossover could reasonable occur.

observed in 2D. Exploring the properties we have discussed above near reentrance in 2D would contribute to the larger picture of studying the role of dimensionality in the state diagram of glasses with attractive interparticle interactions, and would provide further insight into the glass transition. Also, the variation in the average value of the vibrational density of states at low frequencies, i.e., as observed in the transition from repulsive to attractive glasses, has not to our knowledge been considered theoretically. Future theoretical and simulation work on this problem may be useful for clarifying the underlying mechanisms associated with these observations about phonons in glasses.

ACKNOWLEDGMENTS

We thank Wei-Shao Wei and Kevin B. Aptowicz for helpful discussions. M.D.G., X.M., Z.S.D., T.S., and A.G.Y. gratefully acknowledge financial support from the National Science Foundation through Grant No. DMR12-05463, the Penn MRSEC Grant No. DMR11-20901 and its optical microscopy SEF, and NASA Grant No. NNX08AO0G. P.H. gratefully acknowledges financial support from the National Science Foundation through Grant No. RUI-1306990.

M.D.G. and X.M. contributed equally to this work.

[1] F. Sciortino, Nat. Mater. **1**, 145 (2002).
[2] K. A. Dawson, Curr. Opin. Colloid Interface Sci. **7**, 218 (2002).
[3] G. Foffi, C. De Michele, F. Sciortino, and P. Tartaglia, Phys. Rev. Lett. **94**, 078301 (2005).
[4] W. R. Hall and P. G. Wolynes, J. Phys. Chem. B **112**, 301 (2008).
[5] L. Berthier and G. Tarjus, Phys. Rev. Lett. **103**, 170601 (2009).
[6] J. Bergenholtz and M. Fuchs, Phys. Rev. E **59**, 5706 (1999).
[7] A. K. Atmuri, G. A. Peklaris, S. Kishore, and S. R. Bhatia, Soft Matter **8**, 8965 (2012).
[8] D. Marzi, B. Capone, J. Marakis, M. C. Merola, D. Truzzolillo, L. Cipelletti, F. Moingeon, M. Gauthier, D. Vlassopoulos, C. N. Likos, and M. Camargo, Soft Matter **11**, 8296 (2015).
[9] E. Zaccarelli and W. C. K. Poon, Proc. Natl. Acad. Sci. USA **106**, 15203 (2009).
[10] K. N. Pham, S. U. Egelhaaf, P. N. Pusey, and W. C. K. Poon, Phys. Rev. E **69**, 011503 (2004).
[11] L. J. Kaufman and D. A. Weitz, J. Chem. Phys. **125**, 074716 (2006).
[12] A. Latka, Y. Han, A. M. Alsayed, A. B. Schofield, A. G. Yodh, and P. Habdas, Europhys. Lett. **86**, 58001 (2009).
[13] N. B. Simeonova, R. P. A. Dullens, D. G. A. L. Aarts, V. W. A. de Villeneuve, H. N. W. Lekkerkerker, and W. K. Kegel, Phys. Rev. E **73**, 041401 (2006).
[14] C. K. Mishra, A. Rangarajan, and R. Ganapathy, Phys. Rev. Lett. **110**, 188301 (2013).
[15] Z. Zhang, P. J. Yunker, P. Habdas, and A. G. Yodh, Phys. Rev. Lett. **107**, 208303 (2011).
[16] L. Fabbian, W. Götze, F. Sciortino, P. Tartaglia, and F. Thiery, Phys. Rev. E **59**, R1347 (1999).
[17] F. Sciortino and P. Tartaglia, Adv. Phys. **54**, 471 (2005).
[18] K. Dawson, G. Foffi, M. Fuchs, W. Götze, F. Sciortino, M. Sperl, P. Tartaglia, Th. Voigtmann, and E. Zaccarelli, Phys. Rev. E **63**, 011401 (2000).
[19] T. Eckert and E. Bartsch, Phys. Rev. Lett. **89**, 125701 (2002).
[20] E. Zaccarelli, G. Foffi, K. A. Dawson, S. V. Buldyrev, F. Sciortino, and P. Tartaglia, Phys. Rev. E **66**, 041402 (2002).
[21] A. M. Puertas, M. Fuchs, and M. E. Cates, Phys. Rev. Lett. **88**, 098301 (2002).
[22] M. A. Lohr, T. Still, R. Ganti, M. D. Gratale, Z. S. Davidson, K. B. Aptowicz, C. P. Goodrich, D. M. Sussman, and A. G. Yodh, Phys. Rev. E **90**, 062305 (2014).
[23] N. Koumakis and G. Petekidis, Soft Matter **7**, 2456 (2011).
[24] C. L. Klix, F. Ebert, F. Weysser, M. Fuchs, G. Maret, and P. Keim, Phys. Rev. Lett. **109**, 178301 (2012).
[25] C. L. Klix, G. Maret, and P. Keim, Phys. Rev. X **5**, 041033 (2015).
[26] Edited by W. A. Phillips, *Amorphous Solids*, Topics in Current Physics, Vol. 24 (Springer-Verlag, Berlin, Heidelberg, 1981).
[27] K. Chen, W. G. Ellenbroek, Z. Zhang, D. T. N. Chen, P. J. Yunker, S. Henkes, C. Brito, O. Dauchot, W. van Saarloos, A. J. Liu, and A. G. Yodh, Phys. Rev. Lett. **105**, 025501 (2010).
[28] A. Ghosh, V. K. Chikkadi, P. Schall, J. Kurchan, and D. Bonn, Phys. Rev. Lett. **104**, 248305 (2010).
[29] S. Franza, G. Parisi, P. Urbani, and F. Zamponi, Proc. Natl. Acad. Sci. USA **112**, 14539 (2015).
[30] V. Lubchenko and P. G. Wolynes, Proc. Natl. Acad. Sci. USA **100**, 1515 (2003).
[31] E. Stavrou, C. Tsiantos, R. D. Tsopouridou, S. Kripotou, A. G. Kontos, C. Raptis, B. Capoen, M. Bouazaoui, S. Turrell, and S. Khatir, J. Phys.: Condens. Matter **22**, 195103 (2010).
[32] H. Kobayashi and H. Takahashi, J. Non-Cryst. Solids **427**, 34 (2015).
[33] N. Xu, V. Vitelli, A. J. Liu, and S. R. Nagel, Europhys. Lett. **90**, 56001 (2010).
[34] K. Chen, M. L. Manning, P. J. Yunker, W. G. Ellenbroek, Z. Zhang, A. J. Liu, and A. G. Yodh, Phys. Rev. Lett. **107**, 108301 (2011).
[35] A. Ghosh, V. Chikkadi, P. Schall, and D. Bonn, Phys. Rev. Lett. **107**, 188303 (2011).
[36] M. L. Manning and A. J. Liu, Phys. Rev. Lett. **107**, 108302 (2011).
[37] A. Widmer-Cooper, H. Perry, P. Harrowell, and D. R. Reichman, J. Chem. Phys. **131**, 194508 (2009).
[38] A. Widmer-Cooper, H. Perry, P. Harrowell, and D. R. Reichman, Nat. Phys. **4**, 711 (2008).
[39] A. Tanguy, B. Mantisi, and M. Tsamados, Europhys. Lett. **90**, 16004 (2010).
[40] C. Brito and M. Wyart, J. Stat. Mech. (2007) L08003.
[41] K. Sun, A. Souslov, X. Mao, and T. C. Lubensky, Proc. Natl. Acad. Sci. USA **109**, 12369 (2012).
[42] R. Zargar, J. Russo, P. Schall, H. Tanaka, and D. Bonn, Europhys. Lett. **108**, 38002 (2014).
[43] N. L. Green, D. Kaya, C. E. Maloney, and M. F. Islam, Phys. Rev. E **83**, 051404 (2011).
[44] P. Tan, N. Xu, A. B. Schofield, and L. Xu, Phys. Rev. Lett. **108**, 095501 (2012).
[45] X. Wang, W. Zheng, L. Wang, and N. Xu, Phys. Rev. Lett. **114**, 035502 (2015).

[46] M. Wyart, Europhys. Lett. **89**, 64001 (2010).
[47] J. R. Savage and A. D. Dinsmore, Phys. Rev. Lett. **102**, 198302 (2009).
[48] M. D. Gratale, T. Still, C. Matyas, Z. S. Davidson, S. Lobel, P. J. Collings, and A. G. Yodh, Phys. Rev. E **93**, 050601 (2016).
[49] R. Yamamoto and A. Onuki, Phys. Rev. E **58**, 3515 (1998).
[50] D. N. Perera and P. Harrowell, J. Chem. Phys. **111**, 5441 (1999).
[51] P. Yunker, Z. Zhang, and A. G. Yodh, Phys. Rev. Lett. **104**, 015701 (2010).
[52] S. J. Gerbode, D. C. Ong, C. M. Liddell, and I. Cohen, Phys. Rev. E **82**, 041404 (2010).
[53] J. C. Crocker and D. G. Grier, J. Colloid Interface Sci. **179**, 298 (1996).
[54] D. Kaya, N. Green, C. Maloney, and M. Islam, Science **329**, 656 (2010).
[55] S. Henkes, C. Brito, and O. Dauchot, Soft Matter **8**, 6092 (2012).
[56] M. Schindler and A. C. Maggs, Eur. Phys. J. E **34**, 115 (2011).
[57] A. Ghosh, R. Mari, V. K. Chikkadi, P. Schall, A. C. Maggs, and D. Bonn, Physica A **390**, 3061 (2011).
[58] C. A. Lemarchand, A. C. Maggs, and M. Schindler, Europhys. Lett. **97**, 48007 (2012).
[59] A. C. Maggs and M. Schindler, Europhys. Lett. **109**, 48005 (2015).
[60] A. Hasan and C. E. Maloney, Phys. Rev. E **90**, 062309 (2014).
[61] K. Chen, T. Still, S. Schoenholz, K. B. Aptowicz, M. Schindler, A. C. Maggs, A. J. Liu, and A. G. Yodh, Phys. Rev. E **88**, 022315 (2013).
[62] T. Still, C. P. Goodrich, K. Chen, P. J. Yunker, S. Schoenholz, A. J. Liu, and A. G. Yodh, Phys. Rev. E **89**, 012301 (2014).
[63] J. D. Weeks, D. Chandler, and H. C. Andersen, J. Chem. Phys. **54**, 5237 (1971).
[64] J. Taffs, A. Malins, S. R. Williams, and C. P. J. Royall, J. Chem. Phys. **133**, 244901 (2010).
[65] Y. L. Han and D. G. Grier, Phys. Rev. Lett. **91**, 038302 (2003).
[66] J. Baumgartl and C. Bechinger, Europhys. Lett. **71**, 487 (2005).
[67] L. Parolini, A. D. Law, A. Maestro, D. M. A. Buzza, and P. Cicuta, J. Phys.: Condens. Matter **27**, 194119 (2015).
[68] E. R. Weeks, J. C. Crocker, A. C. Levitt, A. Schofield, and D. A. Weitz, Science **287**, 627 (2000).